actuators

MDPI

Article

A Comparative Study of Four Parametric Hysteresis Models for Magnetorheological Dampers

Hongzhan Lv [1,*], Qi Sun [1] and W. J. Zhang [2]

[1] College of Mechanical Engineering, Donghua University, Shanghai 201620, China; 2170714@mail.dhu.edu.cn
[2] Department of Mechanical Engineering, University of Saskatchewan, Saskatoon, SK S7N 5A9, Canada; chris.zhang@usask.ca
* Correspondence: lvhz@dhu.edu.cn

Abstract: The dynamics of the magnetorheological damper is complex, including the inherent hysteresis characteristics and nonlinear creep behavior in the low-velocity region. Mathematical models for these complex dynamics are very important to the function of the damper. In this paper, a comparative study of the four parametric dynamic models, which are the hysteresis bi–viscous model, viscoelastic-plastic model, Bouc–Wen model, and improved Bouc–Wen model, is performed. The study includes the building of a common test apparatus and the parameter identification for the four models. The comparison of the four models concludes that (1) all four models are comparative and that (2) the improved Bouc–Wen model has the highest accuracy.

Keywords: magnetorheological damper; hysteresis characteristic; parametrized model; nonlinear behavior; description accuracy

Citation: Lv, H.; Sun, Q.; Zhang, W.J. A Comparative Study of Four Parametric Hysteresis Models for Magnetorheological Dampers. *Actuators* **2021**, *10*, 257. https://doi.org/10.3390/act10100257

Academic Editors: Ramin Sedaghati and Zongli Lin

Received: 26 July 2021
Accepted: 27 September 2021
Published: 29 September 2021

1. Introduction

Magnetorheological fluid (MRF) is a smart material. Applying an external magnetic field to a magnetorheological fluid changes its viscosity and converts it from a Newtonian fluid to a viscoplastic one within milliseconds. The ability of MRF to resist deformation during a phase change is called magnetorheological damping. Based on this ability, a semi-active control device, i.e., magnetorheological damper (MRD), can change its damping force by changing the intensity of its magnetic field. The MRD has a wide range of applications in the field, such as bridge structures [1], car suspensions [2–4], and prosthetic knee joints [5].

To take advantage of this control property, an accurate dynamic model for MRD is indispensable. Among many models, the Bingham model [6,7] and the nonlinear bi-viscosity model [8] have been widely used due to their simple structure, easy solution, and fewer parameters. However, they are not accurate enough for applications that exhibit a significant creep behavior because these applications act at low velocities. Moreover, they cannot describe the hysteresis and nonlinear characteristics of the magnetorheological damper at low velocities.

The hysteresis bi-viscous model, viscoelastic-plastic model [9], and Bouc–Wen model [10] are known to be able to capture the hysteresis behavior and the nonlinear creep behavior of the magnetorheological damper in the low-velocity region. Wereley et al. [11] compared the Bingham model, the bi-viscous model, and the hysteresis bi-viscous model experimentally. They found that the hysteresis bi-viscous model was significantly better than the other three models, specifically enabling one to capture the hysteresis characteristics of the magnetorheological damper in the low-velocity phase. Snyder et al. [12] compared the hysteresis bi-viscous model with the viscoelastic-plastic model. They found that the damping force prediction error of the viscoelastic-plastic model was smaller than that of the hysteresis bi-viscous model for the dataset for parameter identification but larger than that of the hysteresis bi-viscous model for the dataset for testing. Spencer et al. [13] constructed the improved Bouc–Wen model by adding items for describing the damping

and elastic characteristics. The improved model can better describe the experimental results, and its prediction error is smaller than that of the Bingham and Bouc–Wen models (they cannot describe the hysteresis behavior).

With the recent development of intelligent algorithms, some new models describing the hysteric behavior of MR dampers are proposed. The application of the machine learning method in MR dampers has gained interest in various studies because of the high accuracy in predicting the damping force, especially for control purposes. Bahiuddin et al. [14] proposed a new method using the extreme learning machine (ELM) method to deal with the highly nonlinear behavior of MR dampers. This method is faster than the traditional ANN (artificial neural network) in terms of calculation speed, and the average accuracy of the model prediction is equivalent to that of the ANN model, which shows that, compared with traditional ANN, it has the advantage of reducing the possibility of falling into a local solution. Using the indirect modeling method, Wei et al. [15] proposed a feedforward neural network (FNN) model with different input variables. The results show that the indirect method of the proposed model exhibits a high fidelity in characterizing nonlinear damping forces. Compared with the traditional FNN model, the prediction error in the low-velocity region is significantly reduced. In addition, a novel parametric dynamic model based on the quasi-static (QS) model and a Magic Formula hysteresis multiplier, called the QSMF model [16], is investigated to accurately predict and more meaningfully explain the hysteresis behavior of magnetorheological (MR) dampers. These new dynamic models provide a new perspective for the precise control research of MR dampers.

In this paper, the four parametric hysteresis models, including the hysteresis bi-viscous model, viscoelastic-plastic model, Bouc–Wen model, and phenomenological model, are compared, specifically in terms of their corresponding mechanical characteristic curves, resulting in their accuracy and reliability for the magnetorheological damper. First, we examined the accuracy in restructuring the force versus velocity hysteresis cycle, which is related to the rheology of MR fluid in terms of its shear stress versus shear strain rate. Second, we examined the descriptive accuracy of the damping force-fitting when the four models were reconstructed at a variable velocity, and we further demonstrated the comprehensive errors of the four models under different shear stress versus shear strain rates. It is hoped that this will provide a more suitable model choice for the design of a magnetorheological damper.

2. Experimental Section

The test equipment is shown in Figure 1a. The MR damper RD-8040 manufactured by Lord Corporation was chosen. The damper is compact, suitable for industrial suspension applications, and its continuously variable damping is controlled by the increase in the yield strength of the MR fluid in response to the magnetic field strength. The typically technical data shows that the damper's fast response time is less than 15 milliseconds, and the peak damping force is more than 2440 N, which meets the requirement of the experiment. The loading was based on a sine wave excitation with a frequency of 1 Hz and an amplitude of 5 mm. The applied current is 0 A, 0.2 A, 0.4 A, and 0.6 A, respectively. When the test starts, the software system will record the damping force versus displacement data and the damping force versus velocity data under each current. A total of 864 sets of data were collected, and these data will be ready for the testing of the four parameterized models. The damping force versus displacement and the damping force versus velocity obtained during the steady-state operation of the magnetorheological damper are presented in Figure 1b,c, respectively.

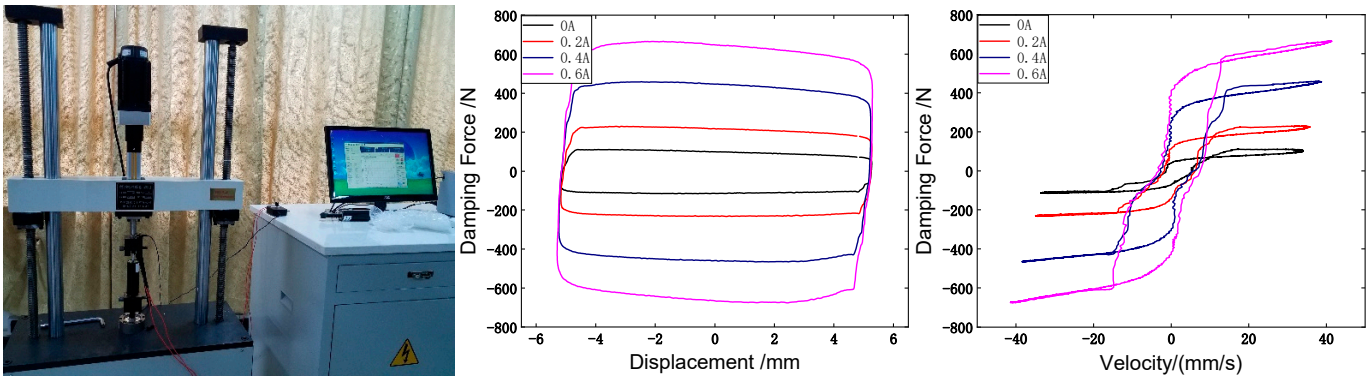

Figure 1. Experiment. (**a**) Test equipment; (**b**) Damping force versus displacement; and (**c**) Damping force–velocity.

In Figure 1b, the damping force versus displacement cycles are approximately rectangular curves. With the increase of the electric current, the maximum value of the damping force corresponding to the different currents steadily increases, and, accordingly, the magnetorheological damper works by producing the damping force. Figure 1c shows that the damping force and velocity exhibit complex nonlinear creep and hysteresis behaviors in the low-velocity region, while their relationship is approximately linear in the high-velocity region. The quality of the models in the low-velocity region was examined for comparison, as the dynamics of the damper show a nonlinear behavior.

3. The Models for Comparison

3.1. Hysteretic Bi-Viscous Model

The bi-viscous model assumes that the magnetorheological fluid is a plastic state in pre-yield and post-yield regions including three parameters, the pre-yield damping coefficient C_{pr}, the post-yield damper coefficient C_{po}, and the yield force F_y, while the pre-yield damping coefficient is much larger than the post-yield damping coefficient. The hysteresis bi-viscous model [17] has one more parameter v_0 than the bi-viscous model, representing the corresponding velocity when the damping force is zero considering the direction of acceleration based on the bi-viscous model. As shown in Figure 2, the relationship between the damping force and velocity in this model is a piecewise linear continuous function. There is an obvious hysteresis cycle in the pre-yield region, a simple linear relationship in the post-yield region, and the hysteretic bi-viscous model itself has apparent symmetry.

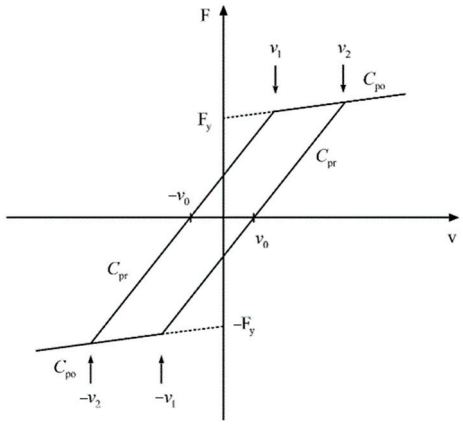

Figure 2. Hysteretic bi-viscous model [17].

The damping force output of the hysteretic bi-viscous model F can be obtained as [17]:

$$F = \begin{cases} C_{po}v - F_y & v \le -v_1 \quad \dot{v} > 0 \\ C_{pr}(v - v_0) & -v_1 \le v \le v_2 \quad \dot{v} > 0 \\ C_{po}v + F_y & v \ge v_2 \quad \dot{v} > 0 \\ C_{po}v + F_y & v \ge v_1 \quad \dot{v} < 0 \\ C_{pr}(v + v_0) & -v_2 \le v \le v_1 \quad \dot{v} < 0 \\ C_{po}v - F_y & v \le -v_2 \quad \dot{v} < 0 \end{cases} \tag{1}$$

where v_1 and v_2. represent the yield velocity while decelerating and accelerating, respectively, and are expressed as:

$$v_1 = \frac{F_y - C_{pv}v_0}{C_{pr} - C_{po}} \; v_2 = \frac{F_y + C_{pr}v_0}{C_{pr} - C_{po}} \tag{2}$$

3.2. Viscoelastic-Plastic Model

Unlike the hysteresis bi-viscous model, the viscoelastic-plastic model [12] assumes that the magnetorheological fluid is a viscoelastic state in the pre-yield region and a plastic state in the post-region. Therefore, the viscoelastic-plastic model is mainly divided into two parts: the pre-yield region and the post-yield region, characterized by the prominent nonlinear hysteresis characteristic in the pre-yield region and a linear relation in the post-yield region. The viscoelastic force in the pre-yield region is described by:

$$F_{ve} = K_{ve}x + C_{ve}v \tag{3}$$

where K_{ve} and C_{ve} represent the stiffness and viscous damping in the pre-yield region, respectively, and the shape function in the post-yield region is given by:

$$S_{ve}(v) = \frac{1}{2}\left[1 - \tanh\left(\frac{|v| - v_y}{4\varepsilon_y}\right)\right] \tag{4}$$

where v_y represents the yield velocity and ε_y represents the smoothing factor of the shape function, which adjusts the shape of the shape function. Now, the damping force in the pre-yield region is:

$$F_{pr} = S_{ve}(v)F_{ve} \tag{5}$$

The viscoplastic force in the post-yield region is calculated by:

$$F_{vi} = C_{vi}v \tag{6}$$

where C_{vi} is the viscous damping in the post-yield region, while the corresponding shape function is given by:

$$S_{vi}(v) = \frac{1}{2}\left[1 + \tanh\left(\frac{|v| - v_y}{4\varepsilon_y}\right)\right] \tag{7}$$

The damping force in the post-yield region is:

$$F_{po} = S_{vi}(v)f_{vi} \tag{8}$$

The damping force in the pre-yield region can be obtained as:

$$F_q = S_c(v)F_c = \tanh\left(\frac{v}{4\varepsilon_c}\right)F_c \tag{9}$$

where F_c represents the yield force and ε_c represents the smoothing factor of the corresponding shape function. Finally, the damping force of the viscoelastic-plastic model can be determined as [12]:

$$F = F_{pr} + F_{po} + F_q \tag{10}$$

3.3. Bouc–Wen Model

The Bouc–Wen model is a relatively simple mathematical model that can describe the magnetorheological damper's hysteresis characteristics and nonlinear creep in the low-velocity region without any need for assumptions on the magnetorheological fluid in the pre-yield and post-yield regions. This model contains a set of parallel elastic elements and damping elements. Figure 3 shows the structure of this model.

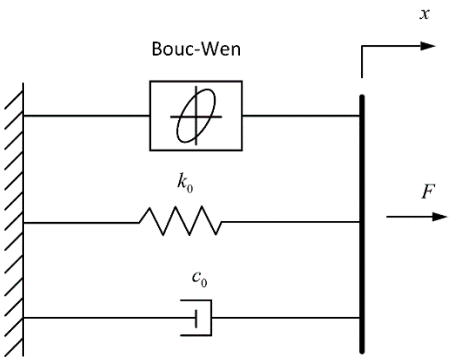

Figure 3. The structure of the Bouc–Wen model [18].

The damping force can be calculated based on the Bouc–Wen model as [18]:

$$F = k_0(x - x_0) + c_0\dot{x} + \alpha z \tag{11}$$

$$\dot{z} = -\gamma|x|z|z|_{n-1} - \beta\dot{x}|z|_n + A\dot{x} \tag{12}$$

where Z is an intermediate variable, k_0 is the stiffness of the spring, x_0 is the initial deformation of the spring, c_0 is the damping coefficient, α is the parameter related to the hysteresis force, γ and β are the parameters related to the shape of the hysteresis cycle, n is the smoothing coefficient of the curve, and A is the coefficient related to the peak value of the damping force.

3.4. Modified Bouc–Wen Model

The modified Bouc–Wen model is a phenomenological model that can be established by adding an elastic element and a viscous element to the Bouc–Wen model. The structure of this model is shown in Figure 4.

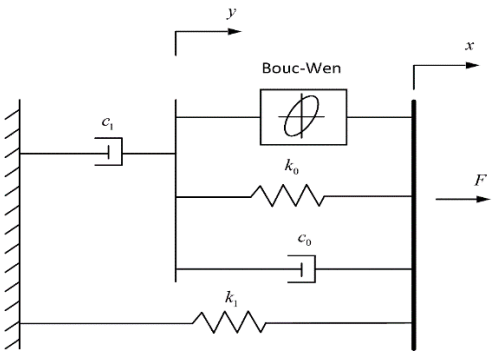

Figure 4. The structure of the improved Bouc–Wen model [13].

The damping force can be obtained based on this phenomenological model as [13]:

$$F = c_1\dot{y} + k_1(x - x_0) \tag{13}$$

where $\dot{y}$ can be expressed as:

$$\dot{y} = \frac{1}{c_0 + c_1}\left[\alpha z + c_0\dot{x} + k_0(x - y)\right] \tag{14}$$

The intermediate variable Z is:

$$\dot{z} = -\gamma|\dot{x} - \dot{y}||z|z|_{n-1} - \beta(\dot{x} - \dot{y})|z|_n + A(\dot{x} - \dot{y}) \tag{15}$$

Among the newly added parameters, c_1 represents the viscous damping coefficient in the low-velocity region and k_1 represents the rigidity of the nitrogen compensator. In the phenomenological model, if the three parameters α, c_0, and c_1 are changed linearly with the applied voltage value, the peak value of the damping force is also changed linearly with the applied current value based on the experimental curve in Figure 1. Therefore, we can assume that the above three parameters change linearly with the applied current value with the following relation:

$$\alpha = \alpha_a + \alpha_b I,\ c_1 = c_{1a} + c_{1b} I,\ c_0 = c_{0a} + c_{0b} I \tag{16}$$

4. Verification and Discussion of Models

4.1. Validation of Models

It is necessary to identify the parameters of all the models. In this paper, the least-square method is employed to identify the parameters of the four models. The function containing the parameter vector is $f(\boldsymbol{p}, \boldsymbol{x})$, where $\boldsymbol{p}$ is the unknown parameter vector, $\boldsymbol{x}$ represents the input to be fitted to the target, the cost function is L, and the target output is y. The principle of the least-square method is to minimize the following cost function (L) by determining the parameter vector:

$$L = \sum_{i=1}^{n}(y_i - f(\boldsymbol{p}, x_i))^2 \tag{17}$$

After obtaining the corresponding parameters for the four parametric models, the models are validated by comparing the results calculated from the models with the experimental results, as shown in Figure 5, (the electric current: 0 A, 0.2 A, 0.4 A, and 0.6 A correspond to Figures 5a, 5b, 5c and 5d, respectively). From Figure 5, it can be seen that the hysteresis bi-viscous model exhibits a strong linear relation in both the low-velocity and high-velocity regions; however, it cannot smoothly transit from the low-velocity region to the high-velocity region. Besides, since the experimental results still have a certain degree of hysteresis in the high-velocity region, the hysteresis bi-viscous model can only linearly fit the high-velocity region of the damping force-velocity curve and cannot characterize the hysteresis in the high-velocity region. Therefore, the hysteresis bi-viscous model has certain limitations. Compared with the hysteresis bi-viscous model, though the viscoelastic-plastic model can describe the nonlinear damping force–velocity relation in the low-velocity region, it cannot describe the hysteresis characteristics in the high-velocity region.

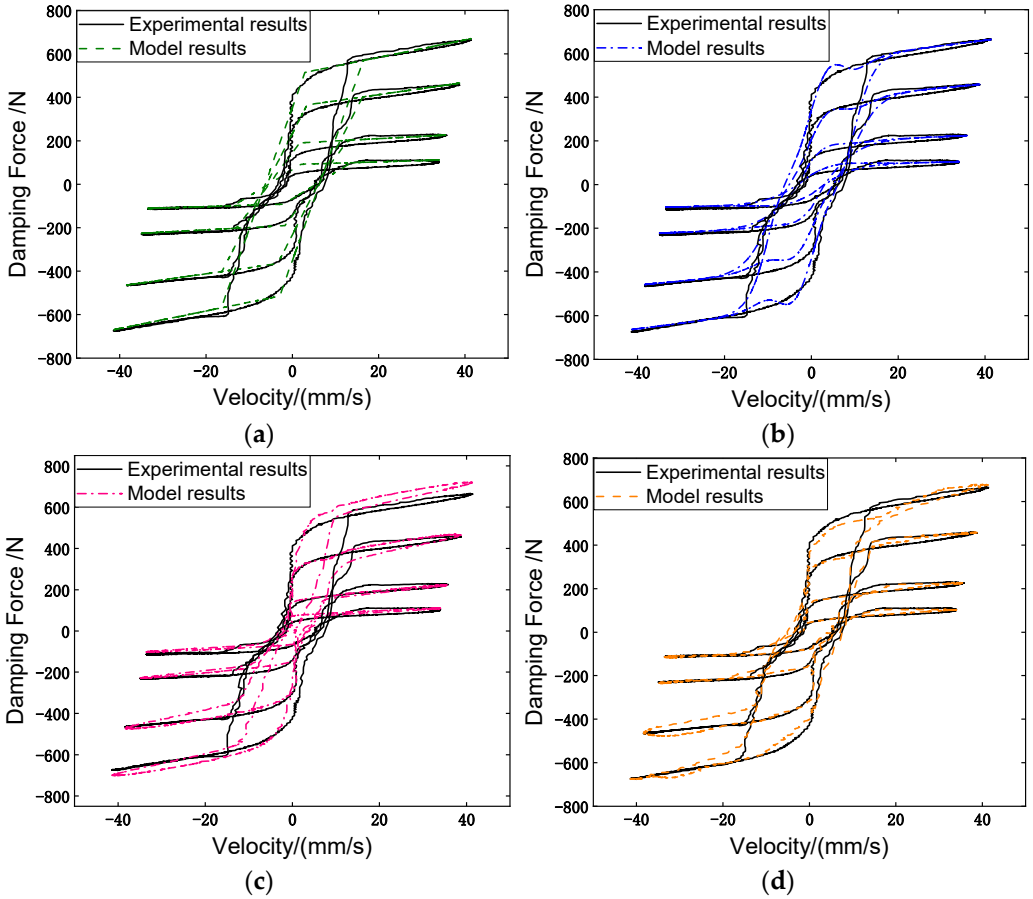

Figure 5. Comparison of the model results with the experimental results. (**a**) Hysteretic bi-viscous model; (**b**) Viscoelastic-plastic model; (**c**) Bouc–Wen model; and (**d**) Modified Bouc–Wen model.

Both the Bouc–Wen model and the modified Bouc–Wen model can achieve the nonlinear fitting in the low-velocity region and describe the hysteresis characteristics in the high-velocity region. However, when the Bouc–Wen model is fitted to a current value of 0.6 A, the width of the hysteresis cycle in the low-velocity region is narrower than the experimental result, while the peak value of the damping force is larger than the experimental result, leading to a more significant fitting error with the Bouc–Wen model for this current. Compared with the other three models, the modified Bouc–Wen model best agrees with the experiment on the hysteresis characteristics in the high-velocity region and nonlinear characteristics in the low-velocity region.

4.2. Comparison of Models

The damping force errors of the four models at different currents are shown in Figure 6. In this figure, $y = 0$ represents a straight line with a damping force error of zero, which is employed as a reference line to evaluate the fitting error of each model; the closer the error line of the model fitting result to the straight line, the higher the fitting accuracy of the model to the experimental result. As shown in Figure 6, since the nonlinear curve in the low-velocity region is more difficult to fit than the linear curve in the high-velocity region, the error in the low-velocity region is more significant than that in the high-velocity region, especially near the low-velocity region with a velocity of zero.

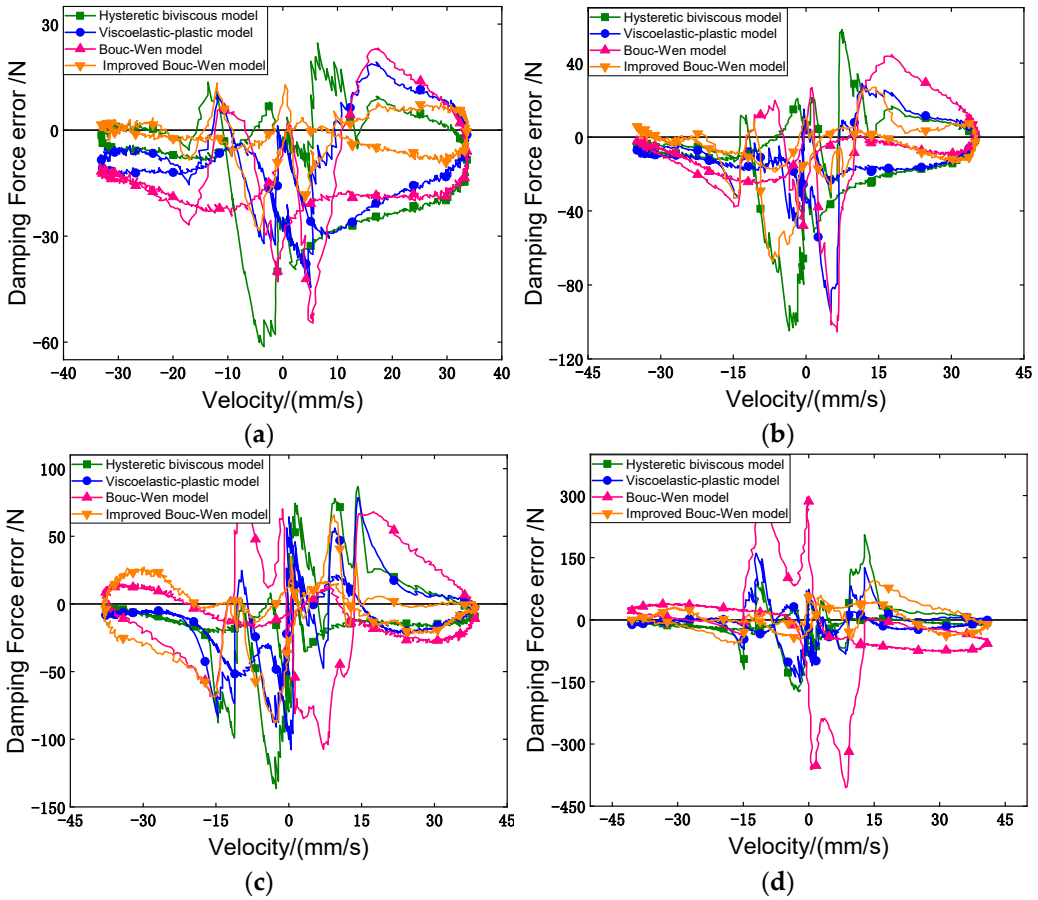

Figure 6. Damping force errors of four models at different current values. (**a**) The damping force error at 0 A; (**b**) The damping force error at 0.2 A; (**c**) The damping force error at 0.4 A; and (**d**) the damping force error at 0.6 A.

Since the hysteresis bi-viscous model is described linearly in the low-velocity region, the prediction accuracy with the model significantly deviates from the experimental results for the nonlinear hysteresis cycle, leading to a higher damping force error in the low-velocity region. For the viscoelastic-plastic model, when the low-velocity region is transiting to the high-velocity region, the velocity reduction described for the damping force is slower than the experimental result, while the hysteresis cycle curve is broader than the experimental curve near the velocity of zero. For the Bouc–Wen model, the hysteresis cycle width of this model in the low-velocity region is narrower than the experimental curve, and the peak value of the damping force at the forward velocity is higher than the experimentally measured damping force. The damping force error curve of the improved Bouc–Wen model under the same excitation current is relatively closer to a straight line than other models with zero error and a higher description accuracy.

From the mechanism of the damping force of the MR damper acting on the magnetic field, it is known that the damping force mainly includes friction damping, viscous damping, shear damping, as well as elastic damping and inertial damping. Among these damping items, friction damping, viscous damping, and shear damping characterize the general trend of the magnetorheological damping force changing with velocity, while the elastic damping and inertial terms, especially the elastic damping, are affected by such nonlinear items as magnetic field changes, temperature changes, and the continuity of the flux linkage. Due to the influence of factors, the damping force is more obviously affected at a low velocity, and it shows an obvious creep behavior when it is hysteretic. The question of how to model the hysteretic behavior at a low velocity and accurately describe the mechanical behavior of the magnetorheological damper in the low-velocity region

constitutes the current difficulty in modeling. Therefore, the fluctuation of the damping force description error with the velocity is caused by the models themselves rather than imperfect measurements. This performance is not random, it is mainly related to the change of material elasticity when the magnetorheological fluid is under the excitation state at a low velocity, and it follows at least a statistical change law.

4.3. Discussion

The literature review shows that these four models are the common and basic models currently used for the dynamic prediction of magnetorheological dampers. In the past two decades, according to the modeling methods that the developed models adopted, the models could be categorized as parametric dynamic models and nonparametric dynamical models. The parametric modeling technique characterizes the device as a collection of linear and/or nonlinear springs, dampers and other physical elements. Various kinds of parametric dynamic models for MR dampers based on mechanical idealizations (mainly including the Bingham-model-based dynamic models, bi-viscous models, viscoelastic–plastic models, stiffness–viscosity elasto-slide models, Bouc–Wen hysteresis operator-based models, Dahl hysteresis operator-based models, LuGre hysteresis operator-based models, equivalent models and so on) have been explored and validated [17]. In this work, these four models with the ability to describe the nonlinear hysteretic behavior in the low-velocity region are the most commonly used and most basic parameterized models, and these models are often modified to adapt to different damper systems. Therefore, that is the reason why these four models were selected for the study.

Although the Bingham model and bi-viscous model cannot describe the hysteresis characteristics and nonlinearity of the magnetorheological damper in the low-velocity region, the two models are simple and provide the inspiration and theoretical basis for the complex high-precision models. For example, the hysteresis bi-viscous model considers the direction of acceleration based on the bi-viscous model and the added parameter v_0 in order to exhibit hysteresis characteristics in the low-velocity region. Moreover, the hysteresis bi-viscous model solves the hysteresis problem in the low-velocity region and is more appropriate for describing the mechanical behavior of magnetorheological dampers than the Bingham model and the bi-viscous model. Besides, it has a better accuracy than the Bingham model and bi-viscous model [11].

The proposed viscoelastic-plastic model employs different assumptions compared with the Bingham model and bi-viscous model, specifically assuming that the magnetorheological fluid is a viscoelastic body in the pre-yield region and a viscoplastic body in the post-yield region, which is a more reasonable assumption than that of the Bingham model and bi-viscous model. Consequently, it provides a higher accuracy than that of the Bingham model and bi-viscous model.

The Bouc–Wen model employs different principles and characteristics to describe the mechanical behavior of magnetorheological dampers using intermediate variables. Spencer et al. [13] improved the Bouc–Wen model and considered three parameters related to the voltage value. The improved Bouc–Wen model agrees with the experimental results more than the other three parametric hysteresis models and considers the relationship between the parameters and current in order to realize the semi-active control of the magnetorheological damper. Therefore, the improved Bouc–Wen model has a higher accuracy, which provides a reference for the subsequent realization of the precise control design of the magnetorheological damper.

In terms of the complexity and time consumption for each model, for most models, though the dynamic models for MR dampers with more parameters possess a better prediction accuracy than those with fewer parameters when the parameters are identified with appropriate methods, the complexity of these models and the consumption of computational resources are also higher due to the increase in parameters. Sahin et al. [19] also provided the idea that the differential parametric models showed no appreciable advantage over the algebraic models at the expense of their complexity and massive time consump-

tion for finding their larger number of model parameters. Based on this perspective, the hysteresis bi-viscous model and the viscoelastic-plastic model have an advantage over the two Bouc–Wen-based models because their models contain more parameters.

In designing magnetorheological dampers, a highly accurate model is required to achieve the precise control of the magnetorheological damper. In the literature, the parametric models for the magnetorheological damper were mainly focused on the Bingham model or the bi-viscous model. Although the accuracy of these two models is not high enough, they can meet the requirements of the general engineering applications of magnetorheological devices. In those applications that have a higher requirement, e.g., flexible robots [16,17], the accuracy of the model that corresponds to the magnetorheological device becomes an issue worthy of attention.

5. Conclusions

In this paper, the mechanical properties of the magnetorheological damper are evaluated through experiments, the parameters of the hysteresis bi-viscous model, viscoelastic-plastic model, Bouc–Wen model, and improved Bouc–Wen model are identified, and the four models are constructed based on the experiment. The following conclusions can be drawn:

(1) The hysteresis bi-viscous model, viscoelastic-plastic model, Bouc–Wen model, and the modified Bouc–Wen model can all approximately describe the hysteresis characteristics of the magnetorheological damper and the nonlinear creep behavior of the piston in the low-velocity region at both ends. Moreover, they can characterize the mechanical behavior of the magnetorheological damper. Among them, the modified Bouc–Wen model can best describe the nonlinear creep behavior in the low-velocity region.

(2) The prediction error of the damping force of the four parametric hysteresis models in the low-velocity region is higher than that in the high-velocity region. The modified Bouc–Wen model provides a more accurate description of the nonlinear creep behavior of the damping force in the low-velocity region and therefore shows promise for the realization of the semi-active control of the magnetorheological damper due to the introduction of the excitation current.

Author Contributions: Conceptualization, H.L.; methodology, H.L. and Q.S.; theoretical analysis, H.L. and Q.S.; validation, H.L. and Q.S.; writing—original draft preparation, H.L. and Q.S.; writing—review and editing, H.L. and W.J.Z.; funding acquisition, H.L. All authors have read and agreed to the published version of the manuscript.

Funding: This research was funded by the Natural Science Foundation of Shanghai, grant number 20ZR1401300.

Institutional Review Board Statement: Not applicable.

Informed Consent Statement: Not applicable.

Data Availability Statement: The data that support the findings of this study are available from the corresponding author upon reasonable request.

Acknowledgments: The authors would like to thank to the Dynamics Laboratory in the College of Mechanical Engineering, Donghua University for the experimental support.

Conflicts of Interest: The authors declare no conflict of interest.

References

1. Weber, F.; Distl, H. Amplitude and frequency independent cable damping of Sutong Bridge and Russky Bridge by magnetorheological dampers. *Struct. Control Health Monit.* **2015**, *22*, 237–254. [CrossRef]
2. Morales, A.L.; Nieto, A.J.; Chicharro, J.M.; Pintado, P. A semi-active vehicle suspension based on pneumatic springs and magnetorheological dampers. *J. Vib. Control* **2018**, *24*, 808–821. [CrossRef]

3. Lindler, J.E.; Dimock, G.A.; Wereley, N.M. Design of a magnetorheological automotive shock absorber. *Proc. Spie Int. Soc. Opt. Eng.* **2000**, *3985*, 426–437.
4. Choi, S.B.; Lee, S.K.; Park, Y.P. A Hysteresis Model for the Field-Dependent Damping Force of a Magnetorheological Damper. *J. Sound Vib.* **2001**, *245*, 375–383. [CrossRef]
5. Xu, L.; Wang, D.-H.; Fu, Q.; Yuan, G.; Hu, L.-Z. A novel four-bar linkage prosthetic knee based on magnetorheological effect: Principle, structure, simulation and control. *Smart Mater. Struct.* **2016**, *25*, 115007. [CrossRef]
6. Occhiuzzi, A.; Spizzuoco, M.; Serino, G. Experimental analysis of magnetorheological dampers for structural control. *Smart Mater. Struct.* **2003**, *12*, 703–711. [CrossRef]
7. Lv, H.; Chen, R.; Zhang, S. Comparative experimental study on constitutive mechanical models of magnetorheological fluids. *Smart Mater. Struct.* **2018**, *27*, 115037. [CrossRef]
8. Sims, N.D.; Holmes, N.J.; Stanway, R. A unified modelling and model updating procedure for electrorheological and magnetorheological vibration dampers. *Smart Mater. Struct.* **2004**, *13*, 100–121. [CrossRef]
9. Li, W.H.; Yao, G.Z.; Chen, G.; Yeo, S.H.; Yap, F.F. Testing and steady state modeling of a linear MR damper under sinusoidal loading. *Smart Mater. Struct.* **2000**, *9*, 95–102. [CrossRef]
10. Ma, X.Q.; Rakheja, S.; Su, C.-Y. Development and Relative Assessments of Models for Characterizing the Current Dependent Hysteresis Properties of Magnetorheological Fluid Dampers. *J. Intell. Mater. Syst. Struct.* **2007**, *18*, 487–502.
11. Wereley, N.M.; Pang, L.; Kamath, G.M. Idealized Hysteresis Modeling of Electrorheological and Magnetorheological Dampers. *J. Intell. Mater. Syst. Struct.* **2016**, *9*, 642–649. [CrossRef]
12. Snyder, R.A.; Kamath, G.M.; Wereley, N.M. Characterization and Analysis of Magnetorheological Damper Behavior Under Sinusoidal Loading. *AIAA J.* **2001**, *39*, 1240–1253. [CrossRef]
13. Spencer, B.F., Jr.; Dyke, S.J.; Sain, M.K.; Carlson, J.D. Phenomenological Model for Magnetorheological Dampers. *J. Eng. Mech.* **1997**, *123*, 230–238. [CrossRef]
14. Bahiuddin, I.; Imaduddin, F.; Mazlan, S.A.; Ariff, M.H.M.; Mohmad, K.B.; Ubaidillah, U.; Choi, S.B. Accurate and fast estimation for field-dependent nonlinear damping force of meandering valve-based magnetorheological damper using extreme learning machine method. *Sens. Actuators A Phys.* **2021**, *318*, 112479. [CrossRef]
15. Wei, S.; Wang, J.; Ou, J. Method for improving the neural network model of the magnetorheological damper. *Mech. Syst. Signal Process.* **2021**, *149*, 107316. [CrossRef]
16. Bui, Q.D.; Bai, X.X.; Hung Nguyen, Q. Dynamic modeling of MR dampers based on quasi–static model and Magic Formula hysteresis multiplier. *Eng. Struct.* **2021**, *245*, 112855. [CrossRef]
17. Wang, D.H.; Liao, W.H. Magnetorheological fluid dampers: A review of parametric modelling. *Smart Mater. Struct.* **2011**, *20*, 023001. [CrossRef]
18. Yi, F.; Dyke, S.J.; Caicedo, J.M.; Carlson, J.D. Experimental Verification of Multiinput Seismic Control Strategies for Smart Dampers. *J. Eng. Mech.* **2001**, *127*, 1152–1164. [CrossRef]
19. Şahin, İ.; Engin, T.; Çeşmeci, Ş. Comparison of some existing parametric models for magnetorheological fluid dampers. *Smart Mater. Struct.* **2010**, *19*, 035012. [CrossRef]